Calhoun: The NPS Institutional Archive

DSpace Repository

Theses and Dissertations 1. Thesis and Dissertation Collection, all items

1954

# Protons, deuterons, and tritons from photonuclear reactions

Wertheim, Robert Halley

Massachusetts Institute of Technology

http://hdl.handle.net/10945/14535

*Downloaded from NPS Archive: Calhoun*

Calhoun is the Naval Postgraduate School's public access digital repository for research materials and institutional publications created by the NPS community. Calhoun is named for Professor of Mathematics Guy K. Calhoun, NPS's first appointed -- and published -- scholarly author.

Dudley Knox Library / Naval Postgraduate School
411 Dyer Road / 1 University Circle
Monterey, California USA 93943

http://www.nps.edu/library

# PROTONS, DEUTERONS, AND TRITONS FROM PHOTONUCLEAR REACTIONS

Robert Halley Wertheim

8854
on spine:

WERTHEIM

1954

THESIS
W47

Letter on front cover:

PROTONS, DEUTERONS, AND TRITONS

FROM PHOTONUCLEAR REACTIONS

Robert Halley Wertheim

# PROTONS, DEUTERONS, AND TRITONS FROM PHOTONUCLEAR REACTIONS

by

ROBERT HALLEY WERTHEIM
B. S., United States Naval Academy
(1945)

SUBMITTED IN PARTIAL FULFILLMENT
OF THE REQUIREMENTS FOR THE
DEGREE OF MASTER OF
SCIENCE
at the
MASSACHUSETTS INSTITUTE OF TECHNOLOGY
June, 1954

## ABSTRACT

Title: "Protons, Deuterons, and Tritons from
Photonuclear Reactions"

Author: Robert H. Wertheim, Lt., U. S. Navy
B. S., U. S. Naval Academy (1945)

Submitted to the Department of Physics on May 21, 1954 in partial fulfillment of the requirements for the degree of Master of Science.

~~25054~~
28844

A scintillation counter telescope has been constructed with which the yields of protons, deuterons, and tritons photoejected from Be, C, and Pb targets by 280 and 140 Mev bremsstrahlung were investigated. Relative yields of the protons, deuterons, and tritons agree with measurements of deuteron-to-proton ratios by De Wire et al(3) if one assumes that the Cornell group did not resolve tritons from deuterons. Differential cross sections for 20 to 40 Mev particles are in reasonable agreement with Levinthal and Silverman(24) considering that the deuterons and tritons seen here were counted as protons in these earlier measurements. The angular distributions of 20 to 40 Mev protons and deuterons show forward asymmetries. Within the experimental uncertainties, the tritons also can have forward angular asymmetry. The percentages of the number of deuterons to the number of protons per unit energy interval at 90° to the beam are 15.8 ± 2.2 for Be, 12.7 ± 2.2 for C, and 19.8 ± 3.1 for Pb. These ratios appear to be proportional to A/Z. Corresponding triton-to-proton ratios are 4.8 ± 1.2, 3.0 ± 1.0, and 5.1 ± 1.5 for Be, C, and Pb, respectively.

All the above observations are consistent with a model wherein the deuterons and tritons are formed by photoprotons and photoneutrons which pick up additional nucleons. Both deuterons and tritons are found, though in somewhat smaller numbers relative to the protons, when the beam energy is reduced to 140 Mev, indicating that mesonic effects alone cannot account for the production of these particles.

Thesis Supervisor:
Jack W. Rosengren
Instructor in Physics
Massachusetts Institute of Technology

TABLE OF CONTENTS

I. Introduction and Theory . . . . . . . . . . . . . . . . . 1

II. Equipment Design and Construction . . . . . . . . . . . . 6

- A. General . . . . . . . . . . . . . . . . . . . . . . . 6
- B. Choice of scintillators . . . . . . . . . . . . . . . 8
- C. Counter construction . . . . . . . . . . . . . . . . 9
- D. Electronics . . . . . . . . . . . . . . . . . . . . . 10

III. Experimental Arrangement and Measurements . . . . . . . 17

- A. Geometry . . . . . . . . . . . . . . . . . . . . . . 17
- B. Measurements . . . . . . . . . . . . . . . . . . . . 19
- C. Mass resolution . . . . . . . . . . . . . . . . . . 21

IV. Reduction of Data and Results . . . . . . . . . . . . . 25

- A. Energy calibration . . . . . . . . . . . . . . . . . 25
- B. Rough data . . . . . . . . . . . . . . . . . . . . . 25
- C. Angular distributions . . . . . . . . . . . . . . . 25
- D. Relative particle yields . . . . . . . . . . . . . . 29
- E. Absolute value of differential cross sections . . . 31
- F. A/Z dependence . . . . . . . . . . . . . . . . . . . 32

V. Conclusions . . . . . . . . . . . . . . . . . . . . . . . 34

VI. Extensions of Present Work . . . . . . . . . . . . . . . 38

VII. Acknowledgment . . . . . . . . . . . . . . . . . . . . 39

VIII. Appendices . . . . . . . . . . . . . . . . . . . . . . 40

IX. Bibliography . . . . . . . . . . . . . . . . . . . . . . 45

# LIST OF ILLUSTRATIONS

| Fig. | | Page |
|---|---|---|
| 1. | Counter No. 1 Construction Detail . . . . . . . . . . | 12 |
| 2. | Counter No. 3 Construction Detail . . . . . . . . . . | 13 |
| 3. | Anticoincidence Counters Construction Detail . . . | 14 |
| 4. | Block Diagram of Electronics . . . . . . . . . . . . | 15 |
| 5. | Calculated Response of Counters to Protons, Deuterons, and Tritons . . . . . . . . . . . . . . . | 16 |
| 6. | Photograph of Experimental Arrangement . . . . . . | 18 |
| 7. | Example of Rough Data Plot . . . . . . . . . . . . . | 20 |
| 8. | Pulse Height Distribution of Particles from Pb . . | 22 |
| 9. | Composite of Data from 24 Runs Showing Resolution of Deuterons and Tritons . . . . . . . . . . . . . . | 24 |
| 10. | Angular Distributions . . . . . . . . . . . . . . . . | 28 |
| 11. | A/Z Dependence . . . . . . . . . . . . . . . . . . . | 33 |

# I. INTRODUCTION AND THEORY

Of the several theories advanced to explain the neutron and proton yields of photonuclear reactions, none predict within several orders of magnitude the large numbers of photodeuterons that have been observed.(1-3) Byerly and Stevens(1) measured the energies and angular distributions of protons, deuterons, and alpha particles, and the energy distribution of neutrons from copper irradiated with 24 Mev betatron bremsstrahlung, identifying the particles by grain density of tracks and their range in photographic emulsions. The ratio of the yields of 2-6 Mev deuterons to 2-13 Mev protons was found to be 0.32 ± 30 percent and they concluded that neither the statistical model(4) which pictures particles evaporating from a compound nucleus, nor a direct nuclear photo-effect(5,6) could account for the high number of deuterons observed. However, Cameron(16) has suggested that a radially polarized deuteron could be favored over a proton in the statistical decay of a compound nucleus. Byerly and Stevens suggested that a "pick-up" process might be responsible for the deuterons and if so, that one would expect to see a few tritons as well. The pick-up mechanism will be described in detail in later paragraphs.

Another early measurement of the relative deuteron to proton yield was made by Smith and Laslett(2) who irradiated

a copper target with 65 Mev bremsstrahlung. Using the measured radius of curvature of tracks produced in the magnetic field of a 12" cloud chamber to identify deuterons and protons, they reported a relative yield of about 0.5 in the energy interval of 1 to 20 Mev. Like the grain density method used by Byerly and Stevens, this technique is relatively insensitive to mass; hence, experimental uncertainties in their measurements were large.

De Wire et al,(3) using a scintillation counter telescope to distinguish deuterons from protons, measured yield ratios at 90° in the laboratory system resulting from bombardment of Ag, Br, Al, Mo, W, C, Cu, and Pb targets with 310 Mev bremsstrahlung. The equipment consisted of two NaI(Tl) crystals which measured quantities proportional to dE/dx and E. The two outputs were multiplied electronically giving a product pulse approximately proportional to $M^{0.8}Z^2E^{0.2}$. Pulse height analysis showed good resolution between proton and deuteron groups. Deuteron-to-proton yield ratios for 40 Mev particles were found to increase with A from 0.12 for C to 0.24 for Pb with 10 percent statistics. Angular distributions of deuterons with 40 Mev mean energy from C, Cu, Ag, and Pb were reported to be roughly the same as those for photoprotons of equal energy. These workers concluded that the A and Z dependence, energy dependence, and the angular distributions of the deuteron yields were suggestive of a $(\gamma,n)$ or $(\gamma,p)$ reaction followed by a pick-up process. No tritons were reported.

The pick-up process suggested by some of these workers may be described as an inverse stripping reaction.(7,8) York,(9) and Hadley and York(10) observed that bombardments of nuclei with 90 Mev neutrons result in an unexpectedly large yield of deuterons with energies of the same order as the incident neutrons, and with angular distributions peaked sharply forward. Selove(11) obtained similar results using a proton beam. The theoretical treatment of Chew and Goldberger(12) which is in reasonably good agreement with the observed data, postulates a sudden rearrangement wherein a proton is transferred from the target nucleus to the passing neutron. It assumes that the probability of producing a deuteron of a particular momentum $\vec{K}$ by an incident neutron with momentum $\vec{k}$ depends simply on the probability of finding a proton of momentum $(\vec{K} - \vec{k})$ in the nucleus.

Recent evidence from (p,t)(13) and (n,t)(14) reactions indicates that the pick-up process may be responsible for a considerable fraction of the triton yields observed, especially when there are two loosely-bound nucleons available in the target nucleus. Thus, the deuterons and possibly tritons observed in photonuclear reactions could be the result of a two-step process; the photo-ejection of a neutron or proton which then picks up one or more partners in escaping from the nucleus. Insofar as the measured cross sections from these experiments can be applied to photodeuterons, there is an order-of-magnitude agreement with the photodeuteron to photoproton ratios seen.

If this is the correct model, one should expect to find deuterons and perhaps tritons with angular and energy dependences following those of the parent neutrons and protons.

Another possible model involves the photodisintegration of a nuclear subunit, such as the pseudodeuteron proposed by Levinger(16) to explain energy spectra and angular distributions of high energy photoprotons. In a similar manner, a disintegration of a pseudo-alpha particle within the nucleus might result in two recoiling deuterons, or a proton and a triton.

When photons with energies above the meson threshold are involved, it appears that many of the observed photonuclear reactions are produced by photons captured by meson-contributed mechanisms. Results of studies(17,18) of stars produced by high energy x-rays in photographic emulsions indicate that they may be produced by the production and reabsorption of mesons inside the nucleus. The resulting nuclear fragments might be expected to include deuterons and tritons, especially since the heavier hydrogen isotopes have been identified in substantial numbers in secondary particles from nuclear interactions of cosmic rays.

Menon and Rochat(19) examined the 15 to 50 Mev particles from cosmic ray stars, using the multiple scattering as a function of residual range in photographic emulsions to differentiate between deuterons, tritons, and protons. The measured emission

ratio from stars corresponding to nuclear excitations of less than 300 Mev was $(d + t)/(p + d + t) = 0.21 \pm 0.08$. This is in agreement with the theoretical treatment of Le Couteur(20) who applied Weisskopf's evaporation model to highly excited nuclei, and included both the effect of thermal expansion of the nucleus on the nuclear barrier and the neutron excess during statistical decay. Good agreement has also been found between observed energy and angular distributions from cosmic ray stars and the predictions of the theory of evaporation from an excited nucleus. Since photomeson production is thought to be a single nucleon process, and meson yields are observed to vary as $A^{2/3}$, one might expect that the numbers of reabsorbed mesons producing stars would vary as $A^{1/3}$.

There are other possible interactions involving mesons, both real and virtual, which could be responsible for photodeuterons or tritons. For example, a high energy photon might interact directly with a two or three nucleon nuclear subunit to form a meson and a recoiling deuteron or triton. The cross sections for such processes should be extremely low, however.

The experiment to be described was undertaken to improve and extend the data available on the photonuclear yields of protons, deuterons, and tritons. Specific requirements included the positive identification of these particles and the measurement of their angular distributions and relative yields, with maximum photon energies both above and below meson threshold.

## II. EQUIPMENT DESIGN AND CONSTRUCTION

### A. General

The principle of simultaneous measurements of energy and specific energy loss (dE/dx) to identify charged particles was chosen over other identification techniques for its ease of instrumentation using scintillation counters and for the relatively good discrimination offered between protons, deuterons, and tritons. In Appendix I it is shown that over a limited energy range the product of dE/dx and E is approximately constant for a given particle, and for particles of the same energy, the ratios of specific ionizations are $\frac{(dE/dx)_{\text{deuteron}}}{(dE/dx)_{\text{proton}}} = 1.66$, and $\frac{(dE/dx)_{\text{triton}}}{(dE/dx)_{\text{proton}}} = 2.23$.

As is indicated schematically in Fig. 4, the counter telescope consisted of four counters. Counters were designated 1, 2, 3, and 4, referring to their sequence in the telescope assembly. To be counted, a particle was required to cause a coincidence in counters No. 1 and No. 3 without causing an anticoincidence in counters No. 2 or No. 4; thus, No. 2 defined the telescope aperture and No. 4 defined maximum range, while Nos. 1 and 3 measured specific energy loss and energy respectively.

The outputs of counters No. 1 and No. 3 were placed in quadrature on the plates of an oscilloscope with any anti-

coincident output from No. 2 or No. 4 flashing a neon bulb. Both scope face and bulb were photographed. Since the product of the outputs of counters No. 1 and No. 3 were approximately constant for a given particle (see Appendix I), the loci of the end points of the scope traces followed a series of hyperbolas, one curve for each type of particle. With a proper selection of amplifier gain, the presentation of the proton, deuteron, and triton hyperbolas could be optimized.

Iso-mass lines for this telescope were calculated using the curves of Aron(21) and are shown in Fig. 5. Energies indicated on the curves refer to particles leaving the target; therefore, to obtain the energy of the particle that was photoproduced, energy lost in the target must be added. For the thin targets used in this experiment and in the energy range considered, mean energies lost in the targets ranged from 2 Mev for 20 Mev protons to 1 Mev for 50 Mev protons.

The upper limits to the curves were set by the stopping power of the back NaI crystal. A particle with energy greater than these maxima would enter the No. 4 anticoincidence counter and would not be recorded.

The theoretical iso-mass lines of Fig. 5, of course, do not indicate the uncertainties in mass resolution expected in an actual experiment. One of the dominant factors affecting resolution of this equipment was statistical fluctuations in the energy lost in the counters by charged particles. It can

be shown that in the thin NaI(Tl) crystal this Landau-Symon effect(22) was quite important and was of the order of ±9 percent. Statistical fluctuations in photomultiplier photocathode and dynode multiplication contributed an additional ±5 percent in the front counter. Variations in phototube voltages, although held to ±0.2 percent, may account for variations of ±1.4 percent in overall tube gains. In addition, very large effects could be contributed by imperfections in the crystals and nonuniform light collection. Uniformity of the useful area of counter No. 3 was measured to be ±5 percent using a collimated beta source; however, small variations in the thin crystal of counter No. 1 could be much more important. Thus, an overall uncertainty in measurements of dE/dx less than ±10.4 percent was not expected. Since $m \sim (dE/dx)^{1.27}$, this meant a minimum uncertainty in mass resolution of ±13.2 percent.

## B. Choice of scintillators

Sodium iodide, thallium-activated, was chosen as the scintillator for both dE/dx and E measurements because of its linear response. In Appendix II, this choice is supported by a comparison with the potential mass discrimination available using anthracene. NaI(Tl) has a conversion efficiency of ~8.4 percent (conversion efficiency $C \equiv \frac{(h\nu_p)n_p}{\Delta E}$ where

$(h\nu_p)$ is average photon energy, $n_p$ is number of photons emitted, and $\Delta E$ is energy lost in the crystal by the charged particle), and is highly transparent to its own radiation which peaks at 4100 Å. Its emission spectrum is very well matched by the cathode frequency response of available photomultipliers. The disadvantages of NaI(Tl) over other scintillators are its relatively slow (0.25 μsec) decay time and its deliquescence. The latter property posed special design problems for the counters.

The anticoincidence counters which defined solid angle and energy range accepted by the telescope had no such restrictions on linearity of response imposed on No. 1 and No. 3; therefore, plastic scintillators were chosen for them. The plastic was polyvinyltoluene with terphenyl added, commercially available as Pilot B from Pilot Chemical Co. Individual counter construction details are shown in Figs. 1, 2, and 3.

## C. Counter construction

In the manufacture of the thin crystal for counter No. 1, use was made of the deliquescence of NaI. A 1" O.D., 1/8" thick NaI wafer purchased from Tracerlab was placed in a jig consisting of a 20 mil thick celluloid pattern cemented to a lucite block. The crystal was reduced to the thickness of the celluloid by wiping it with a wet cloth stretched over a flat board. It was then placed in a dry box where the excess

moisture was removed by alternately dipping into glycerine and wiping it off. The finished crystal was measured to be 176.7 ± 4 percent mg/cm$^2$. It was sealed into counter No. 1 to which was attached a side arm containing $P_2O_5$ drying agent. The crystal was secured to the front counter window by small strips of scotch tape. As may be seen from Figs. 1 and 4, it was viewed at an angle of 45° by its photomultiplier. This configuration was chosen to maximize light collection at the photocathode with a minimum of stopping power in the first counter.

The large NaI crystal for counter No. 3 was prepared by placing it in a lathe and reducing its diameter to 3 7/8" by rubbing the turning crystal with a wet cloth stretched over a board. It was then placed in a dry box and sealed into its counter to which, like No. 1, a container of $P_2O_5$ was attached. The finished crystal had a measured thickness of 4172.4 mg/cm$^2$.

The construction of counters No. 2 and No. 4 presented no particular problems and can be followed from an examination of Fig. 3.

### D. Electronics

A block diagram of the equipment is shown in Fig. 4. Output signals from the cathode followers were shaped to square pulses by delay line clippers and amplified by linear Model 501 amplifiers. Outputs from the No. 1 and No. 3

amplifiers were delayed for 1 $\mu$sec and then placed on the y and x plates of the oscilloscope. Undelayed output signals which were above levels set on the Schmidt discriminators, in coincidence with each other and with a 2000 $\mu$sec gate triggered by the synchrotron peaking strip, triggered a blocking oscillator the output of which intensified the oscilloscope. Any signal from counters No. 2 or No. 4 in coincidence with the output of this blocking oscillator flashed a neon anticoincidence light which was photographed along with the oscilloscope trace on 16 mm Kodak Linagraph Pan film.

The camera used was a Bell and Howell with f/1.5 lens. In order to obtain the necessary intensity to make the photographic process possible, an oscilloscope was constructed with a 5XP11 cathode-ray tube operating at 12 kev. Continuous film drive was provided by an electric motor coupled to the camera through a reduction gear. The motor speed was adjusted to the No. 1 and No. 3 coincidence counting rate in order to prevent excessive overlap of traces. X and Y axes were photographed at least once on each film roll and were used to provide a reference when measuring the pulse coordinates.

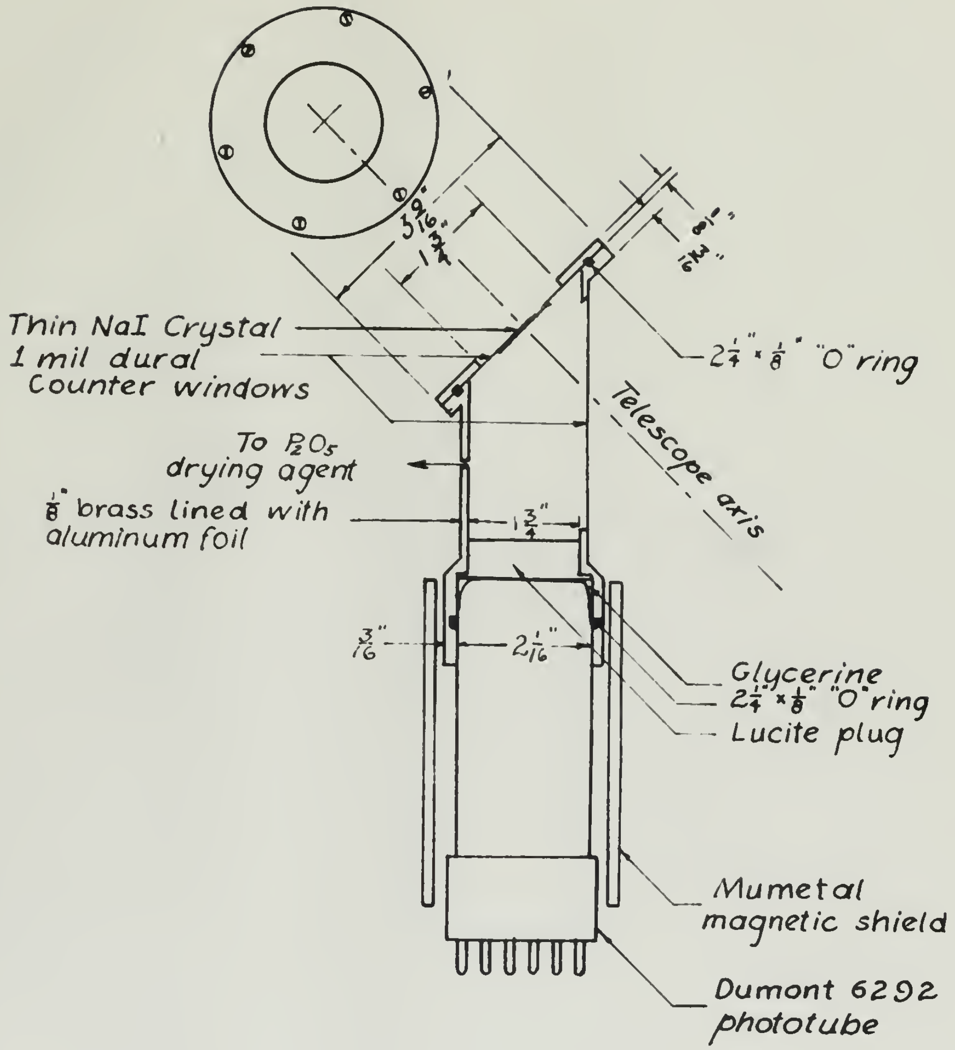

Figure 1

Counter No. 1 Construction Detail

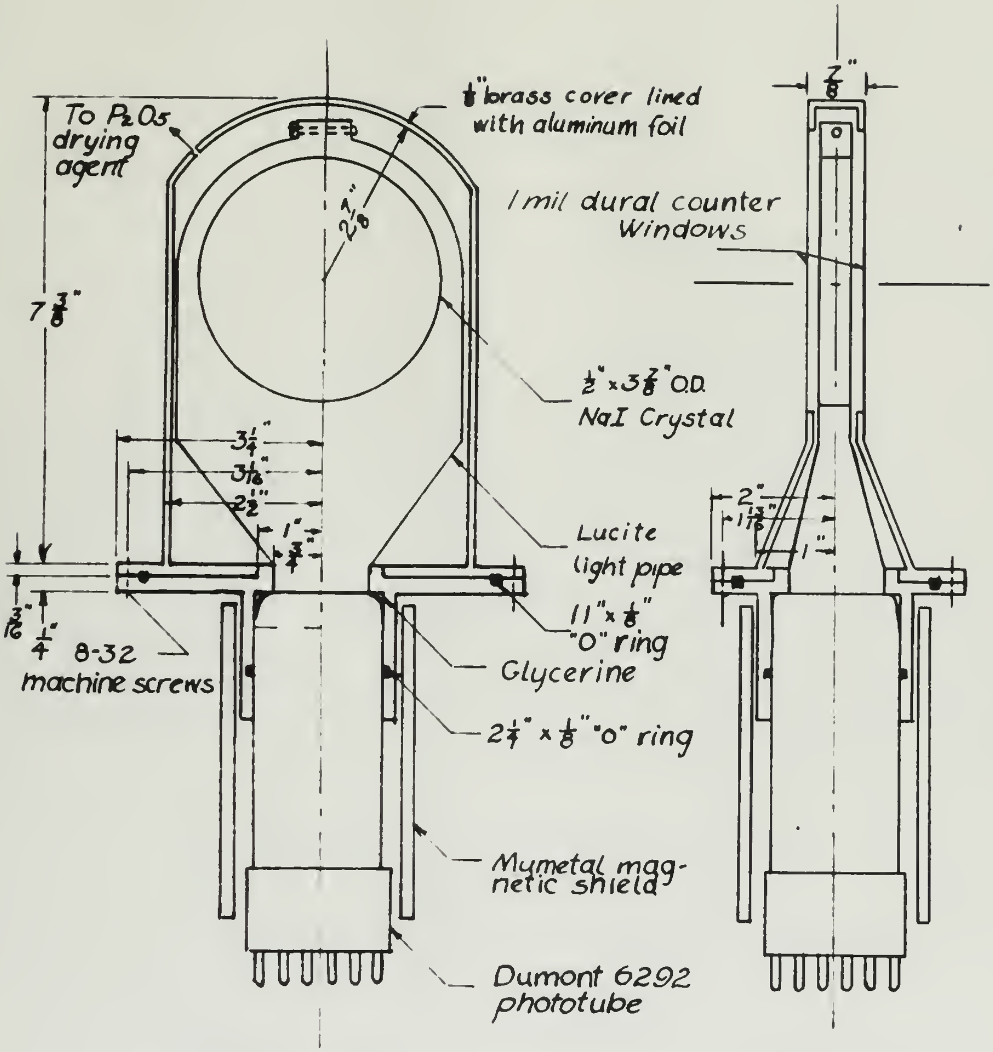

Front View

Side View

Figure 2

Counter No. 3 Construction Detail

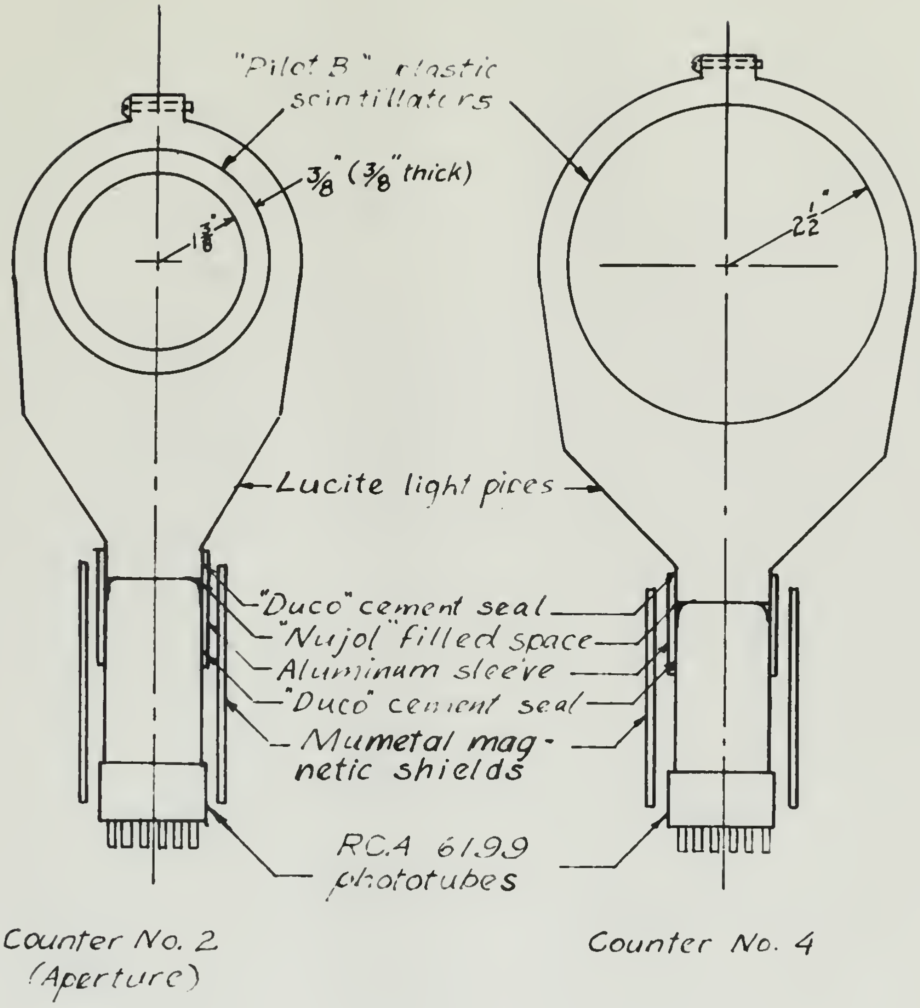

Figure 3

Anticoincidence Counters Construction Detail

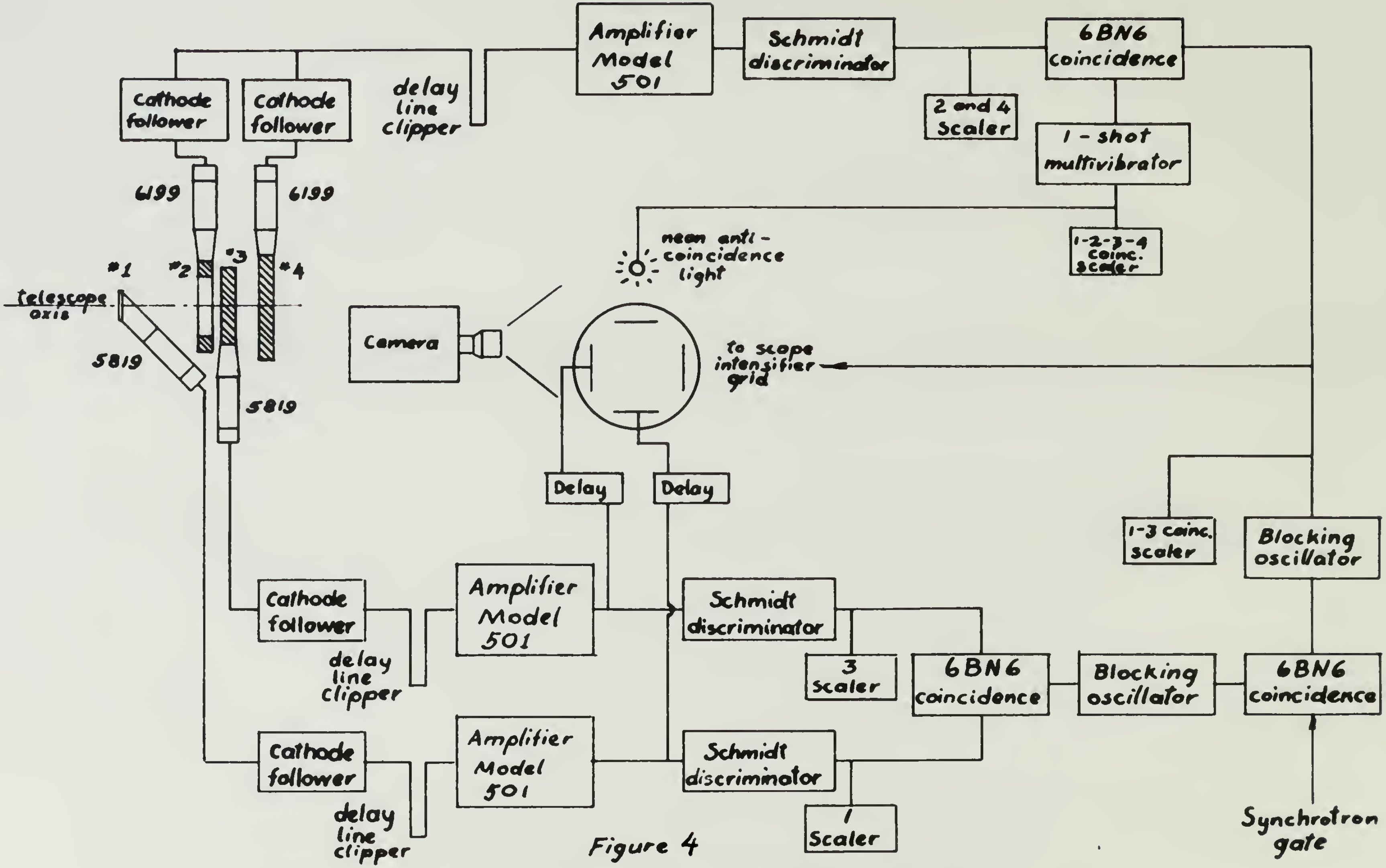

Figure 4

Block Diagram of Electronics

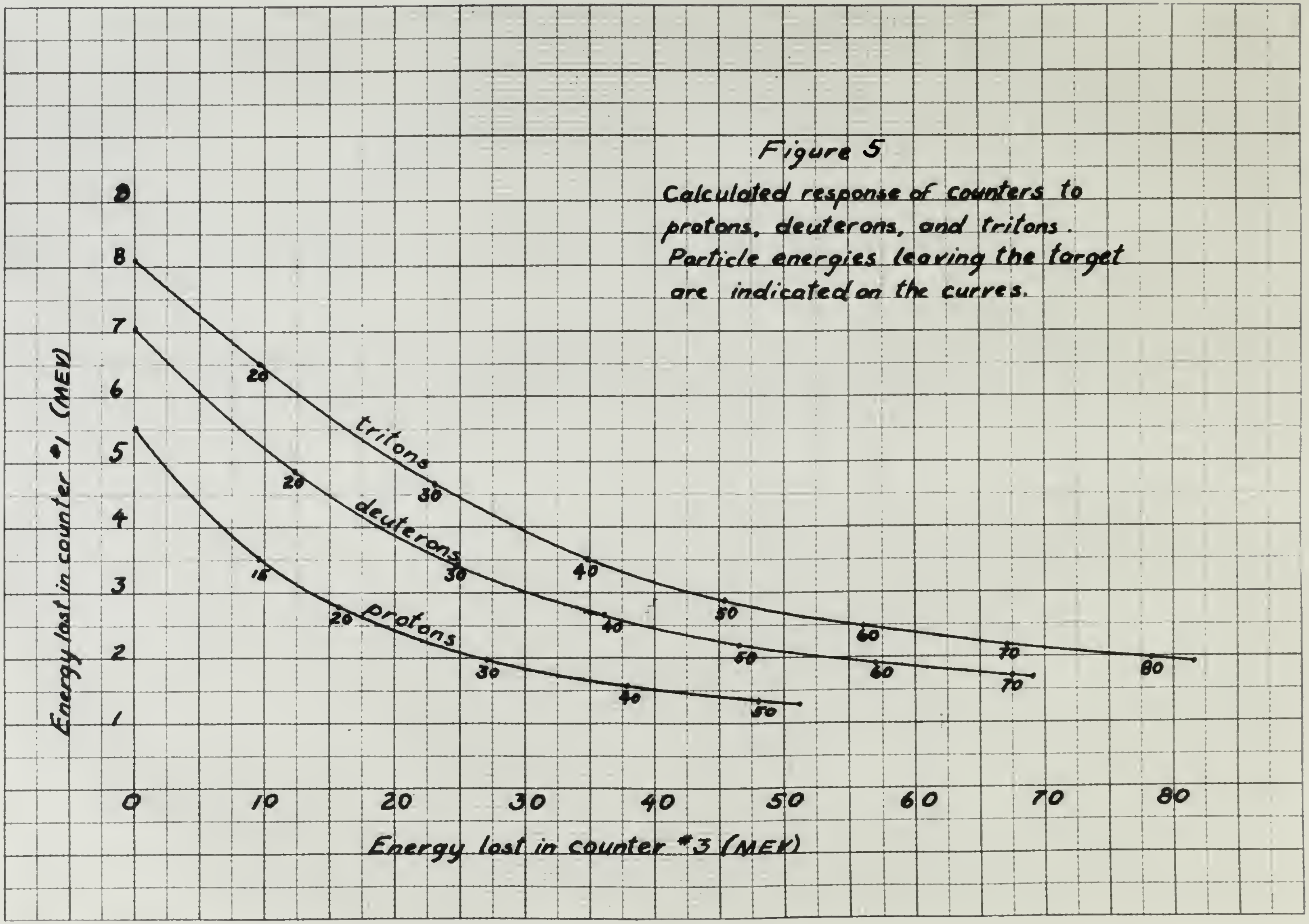

Figure 5

Calculated response of counters to protons, deuterons, and tritons. Particle energies leaving the target are indicated on the curves.

# III. EXPERIMENTAL ARRANGEMENT AND MEASUREMENTS

## A. Geometry

Figure 6 is a photograph of the apparatus as arranged for this experiment. The counters of the telescope were mounted on a 5/8" plywood base and the assembly was aligned to a common horizontal axis. The base was then securely bolted to a steel turntable.

The target holder consisted of a frame of thin lucite which was held at an angle of 45° to the beam by a rod through the turntable axis. The center of the target frame was aligned optically with the telescope axis, 8 inches from the front counter. Beam position and collimation were checked by exposure of Polaroid Land Camera film at the target position. Each of the thin targets used, 149.19 $mg/cm^2$ Be, 103.8 $mg/cm^2$ C, and 270.8 $mg/cm^2$ Pb, had substantially larger areas than the beam, whose diameter was approximately 1 5/8" at the target center. The position of the lead shielding was adjusted to minimize background counting rate each time the turntable angle was changed.

With the arrangement described, the angular resolution of the telescope was defined by the anticoincidence aperture (counter No. 2), and was estimated to be ±2.3° at 90° and ±2.7° at 45° and 135°. In making angular changes the targets

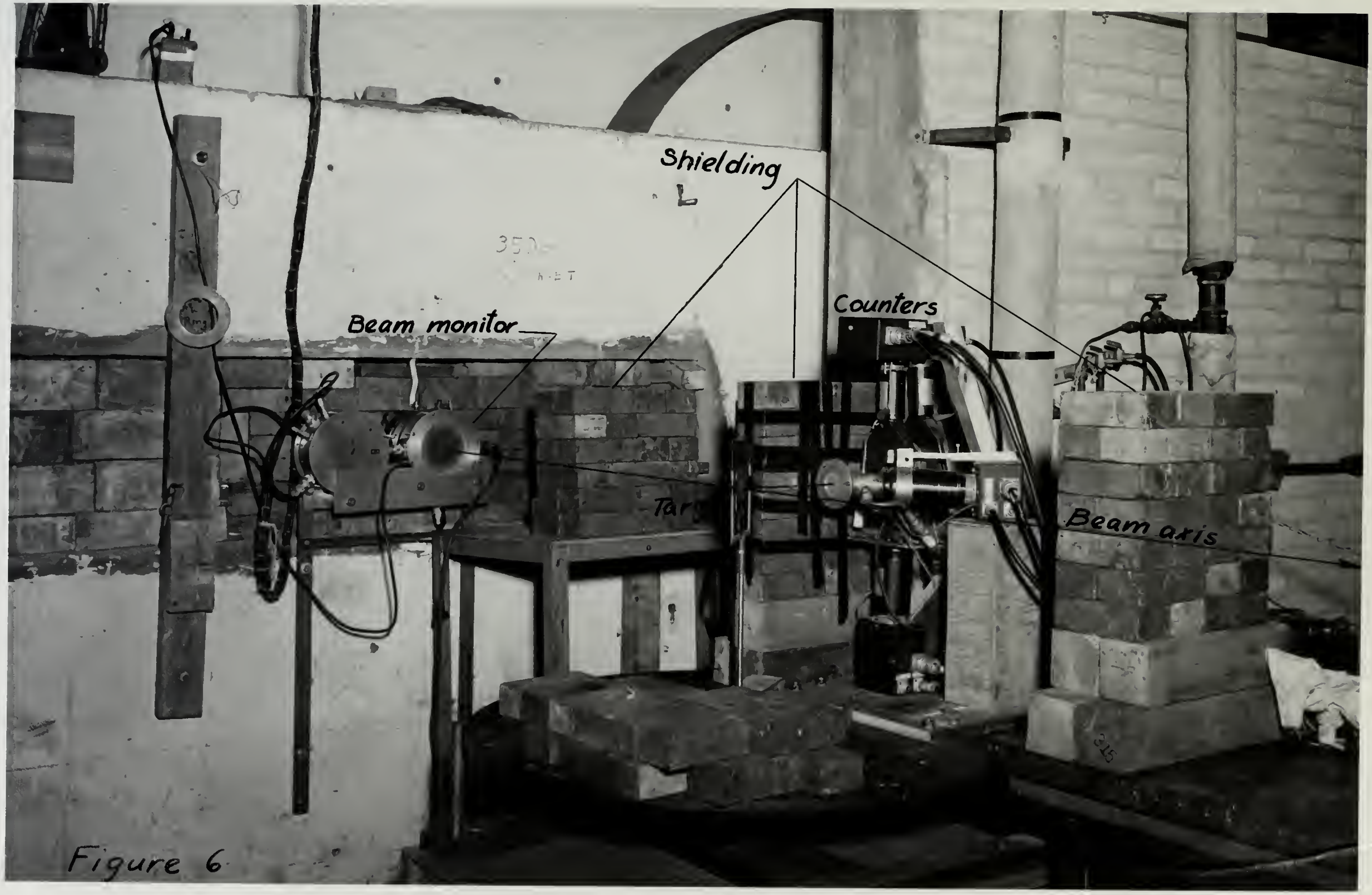

Figure 6

were held fixed at an angle of $45^{\circ}$ to the beam, so that the effective target thicknesses were increased by a factor of $\sqrt{2}$ over the values listed above.

## B. Measurements

The major portion of the measurements were made with a maximum beam energy of 280 Mev. At least two runs were made on each target at $45^{\circ}$, $90^{\circ}$, and $135^{\circ}$ to the beam as well as a no-target run for background at each angle. In addition, several runs were made on the Pb target at $90^{\circ}$ using a beam energy of 140 Mev.

Final data were read from the developed film by projecting in a microfilm viewer. Coordinates of the end points of traces not accompanied by an anticoincidence pulse were plotted as shown in Fig. 7. Principally with the Pb target, some short traces falling inside $x = 3$, $y = 3$ were seen. These were probably electrons or mesons and were not plotted. There were, in addition, a few traces not plotted whose random shapes indicated that they were due to accidental coincidences. It was found that some of the traces with y coordinates less than about 1.8 had no identifiable origins. This was attributed to jitter in firing the multivibrator of the No. 1 discriminator, and undoubtedly resulted in the loss of some of the more energetic protons. For this reason, no proton data were analyzed beyond $x = 13$, corresponding to about 40 Mev.

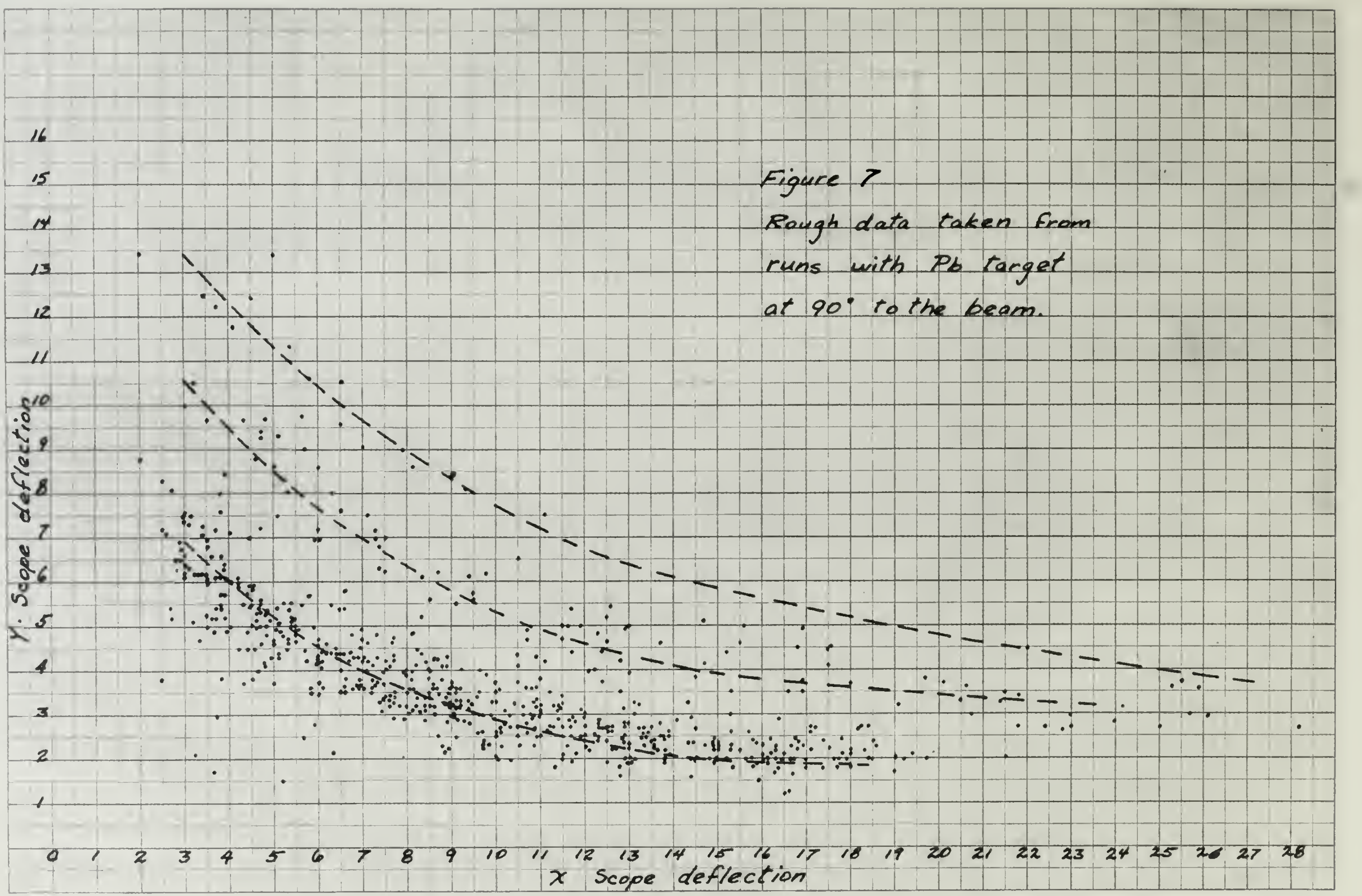

Figure 7
Rough data taken from
runs with Pb target
at 90° to the beam.

A few traces with large y deflections having end points off the scope were seen in all runs except those at 1/2 beam energy. These could have been from multiply charged nuclear fragments, possibly $He^4$ or $He^3$ nuclei.

C. Mass resolution

By normalizing the observed data of Fig. 7 to the theoretical curves of Fig. 5, one obtains a mass scale from which the pulse height distribution of Fig. 8 was plotted. As may be seen from this figure, there are clearly three groups of particles corresponding to protons, deuterons, and tritons. The proton mass is resolved to ±20 percent, not much poorer than the theoretical maximum of ±13.2 percent which was computed earlier.

In Appendix III, it is shown that the statistical mass resolution $\Delta m$, for any singly charged particle relative to that for the protons $\Delta m_p$, is $\frac{\Delta m}{\Delta m_p} = (\frac{m}{m_p})^{0.64}$. With $\Delta m_p = 0.2$ mass units, corresponding standard deviations in mass for deuterons and tritons are

$$\Delta m_d = 0.2(2)^{0.64} = 0.31$$

and

$$\Delta m_t = 0.2(3)^{0.64} = 0.40.$$

Thus, considerable overlap of the tails of the deuteron and triton distributions is to be expected; however, the resolution

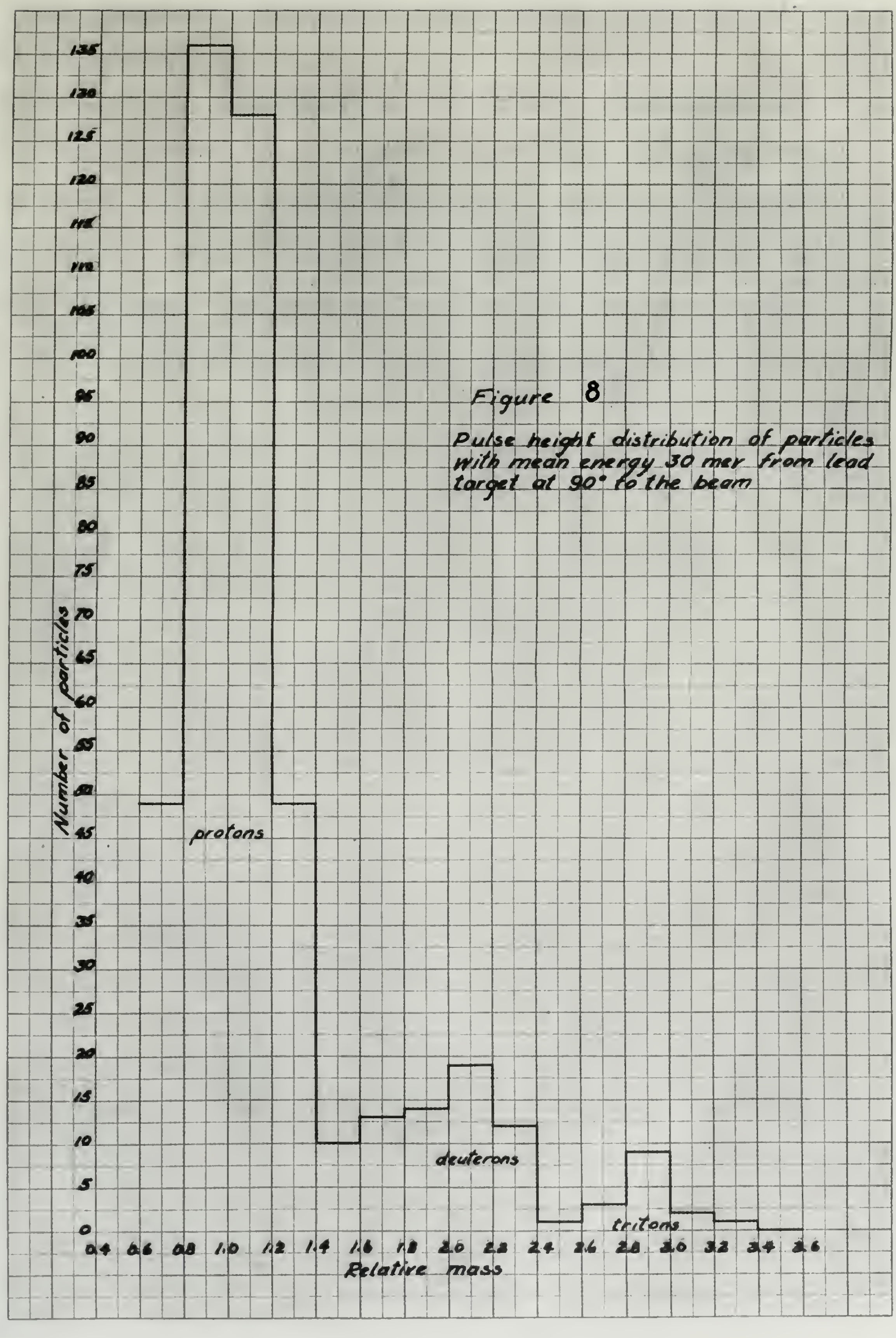

Figure 8

Pulse height distribution of particles with mean energy 30 mev from lead target at 90° to the beam

should be sufficient to permit a reasonable separation of these particles.

Figure 9 is a composite of 24 runs on all targets at all angles, plotted to show mass resolution between deuterons and tritons with numbers large enough to give good statistics. Although small variations in amplifier gains and tube voltages between runs tend to wash out the valley between deuterons and tritons, the separation is still distinct.

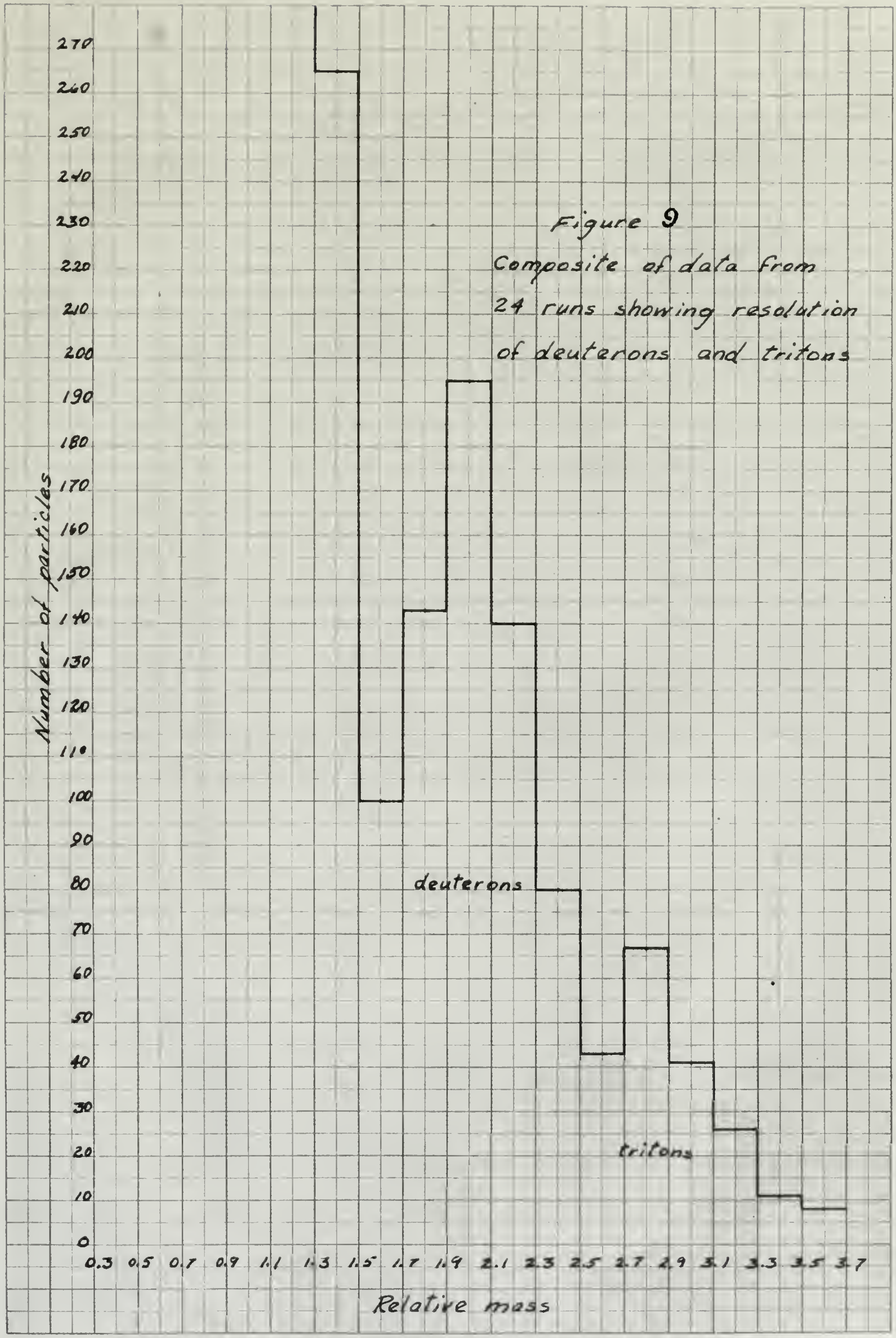

Figure 9

Composite of data from 24 runs showing resolution of deuterons and tritons

## IV. REDUCTION OF DATA AND RESULTS

### A. Energy calibration

Calibration of the energy scale was made by identifying the proton end point at x = 18.3 with the calculated value of 51.1 Mev shown in Fig. 5 for protons which just got through counter No. 3. Because of the loss of higher energy protons into the No. 1 discriminator bias discussed earlier, the useful energy range for comparative particle yields was limited to 20-40 Mev.

### B. Rough data

The numbers of traces counted in each particle group as well as those traces not accepted for reasons discussed in the preceding section are summarized in Table 1. Yields in the energy groups 20-30 Mev, 30-40 Mev, and 20-40 Mev calculated for equal beam monitor readings and corrected for background are listed in Table 2 with corresponding standard deviations.

### C. Angular distributions

The variations in yields with angle have been plotted for protons, deuterons, and tritons in Fig. 10. Values at 45° and 135° are plotted relative to the values measured at 90°. The errors on the curve are statistical. There is general

# Table 1.

| | | | Particles identified 20-40 Mev | | | Traces not counted - all energies | | |
|---|---|---|---|---|---|---|---|---|
| | Target | Exposure (mice)* | p | d | t | Shape | No origin | Off scope |
| Full beam energy | Be 45° | 100 | 199 | 27 | 7 | 9 | 24 | 1 |
| | | 310 | - | 67 | 17 | - | - | 9 |
| | 90° | 432 | 437 | 79 | 23 | 3 | 43 | 5 |
| | 135° | 192 | 155 | 22 | 11 | 3 | 20 | 2 |
| | | 251 | - | 40 | 13 | - | - | 2 |
| | C 45° | 101 | 165 | 22 | 5 | 7 | 19 | 6 |
| | | 170 | - | 23 | 17 | - | - | 4 |
| | 90° | 328 | 389 | 50 | 11 | 8 | 26 | 5 |
| | 135° | 201 | 134 | 14 | 7 | 0 | 17 | 1 |
| | | 549 | - | 47 | 16 | - | - | 4 |
| | Pb 45° | 42 | 67 | 13 | 2 | 7 | 11 | 5 |
| | | 60 | - | 23 | 6 | - | - | 6 |
| | 90° | 228 | 285 | 56 | 14 | 19 | 46 | 5 |
| | 135° | 128 | 134 | 28 | 6 | 6 | 22 | 4 |
| | | 170 | - | 29 | 6 | - | - | 3 |
| | Back-ground | | | | | | | |
| | 45° | 100 | 22 | 4 | 1 | 2 | 1 | 0 |
| | 90° | 109 | 6 | 1 | 0 | 1 | 2 | 0 |
| | 135° | 80 | 4 | 1 | 0 | 0 | 0 | 0 |
| 1/2 energy | Pb 90° | 119.5 | 79 | 9 | 1 | 10 | 0 | 0 |

* 1 mouse = $1.16 \times 10^8$ eq. quanta

Table 2. Particle yields per 100 mice corrected for background.

| | 20-30 Mev | | | 30-40 Mev | | | 20-40 Mev | | |
|---|---|---|---|---|---|---|---|---|---|
| | p | d | t | p | d | t | p | d | t |
| Be 45° | 119<br>± 10.22% | 10.65<br>± 23.7% | 2.17<br>± 61.4% | 58.0<br>±14.8% | 8.27<br>± 21.8% | 2.68<br>±36.3% | 177<br>±8.42% | 18.9<br>± 14.55% | 4.85<br>± 32.1% |
| 90° | 67.6<br>± 8.33% | 9.26<br>±18.55% | 3.93<br>± 28.0% | 42.4<br>±8.17% | 8.10<br>±19.27% | 1.39<br>±56.8% | 110.0<br>±5.01% | 17.4<br>± 13.1 % | 5.32<br>± 23.5% |
| 135° | 39.8<br>± 12.77% | 8.23<br>± 22.5% | 3.61<br>± 30.7% | 37.0<br>±11.9% | 4.51<br>±22.4 % | 1.81<br>±35.4% | 76.8<br>±8.78% | 12.8<br>± 16.39% | 5.42<br>± 23.5% |
| C 45° | 86.0<br>± 12.42% | 6.96<br>± 37.1% | 1.58<br>± 88.4% | 56.4<br>± 1.5% | 5.64<br>± 32.9% | 5.54<br>±27.6% | 142.3<br>±9.6 % | 12.60<br>± 22.6 % | 7.12<br>± 28.0% |
| 90° | 73.7<br>± 6.83% | 8.84<br>± 22.3% | 2.44<br>± 42 % | 39.0<br>±8.66% | 5.49<br>± 27.1% | 0.915<br>±83.2% | 112.7<br>±5.69% | 14.3<br>± 16.5 % | 3.35<br>± 34.3% |
| 135° | 37.8<br>± 12.9 % | 4.08<br>± 34.3% | 2.13<br>± 38.8% | 20.3<br>±14.5% | 2.80<br>± 21.8% | 0.934<br>±37.8% | 61.7<br>±8.69% | 6.88<br>± 22.2 % | 3.06<br>± 29.5% |
| Pb 45° | 64.6<br>± 10.3 % | 18.6<br>± 26.5% | 1.94<br>±101.8% | 73.0<br>±11.2% | 12.7<br>± 30.0% | 4.90<br>±46.4% | 137.5<br>±14.6% | 31.3<br>± 18.4 % | 6.84<br>± 43.1% |
| 90° | 67.3<br>± 8.6 % | 11.8<br>± 21.6% | 4.82<br>± 32.3% | 52.1<br>±9.63% | 11.8<br>± 20.3% | 1.31<br>±71.6% | 119.5<br>±6.49% | 23.7<br>± 14.5 % | 6.14<br>± 28.4% |
| 135° | 46.6<br>± 14.0 % | 10.2<br>± 22.1% | 2.01<br>±51.75% | 53.1<br>±12.1% | 7.72<br>± 20.9% | 2.01<br>±41.0% | 99.7<br>±9.23% | 17.9<br>± 15.5 % | 4.02<br>± 33.1% |
| Pb 90° 1/2 energy | 41.0<br>± 14.3% | 2.51<br>± 57.9% | 0 | 25.1<br>±18.3% | 5.02<br>± 41.6% | 0.84<br>±100 % | 66.1<br>±11.8% | 7.53<br>± 33.0 % | 0.84<br>±100 % |

Figure 10

Angular distributions normalized to 90°
20-40 Mev particles

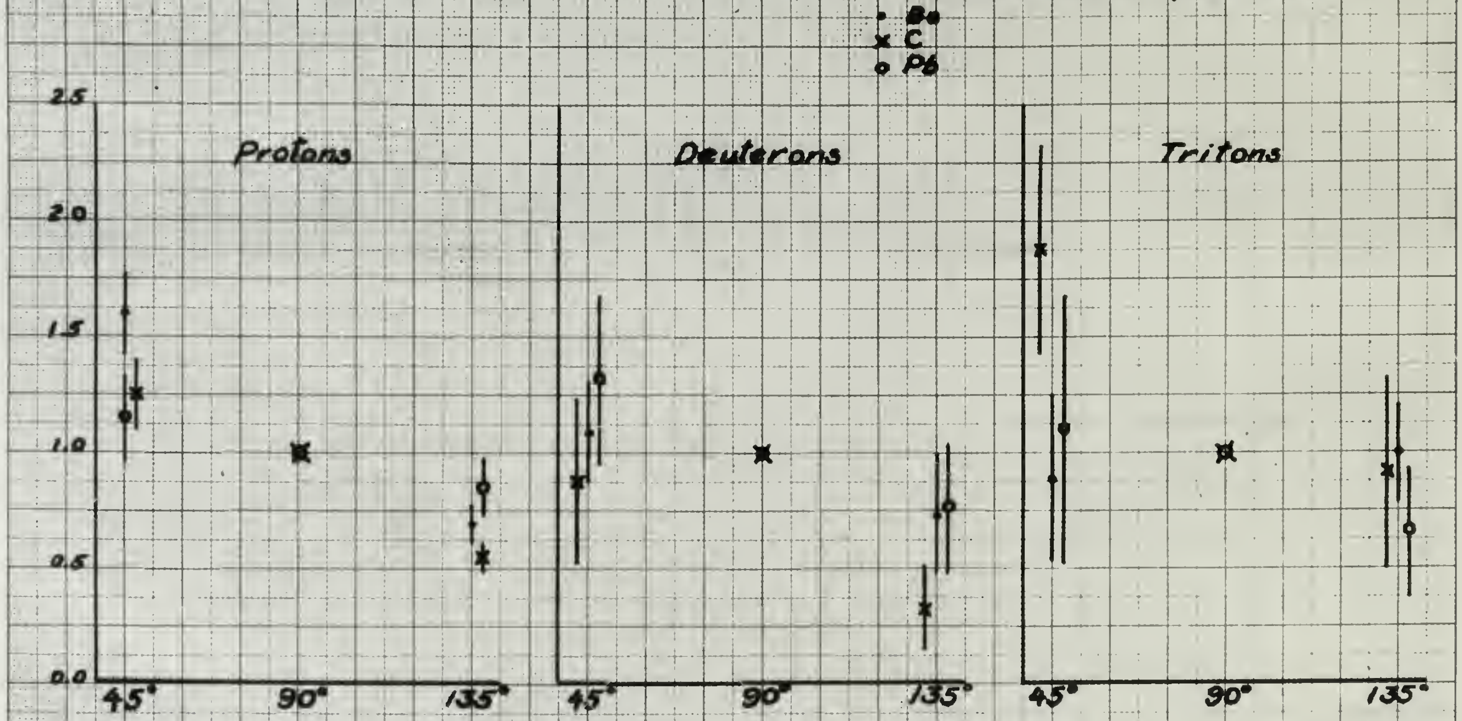

agreement in the proton angular distribution with that reported by Levinthal and Silverman(24) for 40 Mev protons. Within the standard error, the deuteron distribution also shows forward asymmetry as reported by De Wire.(3) Although the uncertainties are quite large in the triton measurements, there is some indication of forward asymmetry here also.

## D. Relative particle yields

The observed deuteron-to-proton (d/p) and triton-to-proton (t/p) yield ratios corrected for background are summarized in Table 3. Errors listed are standard deviations due to counting statistics only. These data are in reasonable agreement with those of De Wire,(3) particularly if one assumes that the triton yields here observed were counted as deuterons by the Cornell group. The figures below compare the net ratios measured here for deuterons and tritons at 90° with the d/p values reported by De Wire.

| | This experiment<br>(d/p + t/p) × 100 | De Wire<br>d/p × 100 |
|---|---|---|
| Be | 20.6 ± 2.5 | 21 ± 2.1 |
| C | 15.7 ± 2.4 | 12 ± 1.2 |
| Pb | 24.9 ± 3.4 | 24 ± 2.4 |

d/p and t/p ratios appear to be somewhat lower for the run at half beam energy, although the statistical uncertainties are very large, especially for the tritons.

Table 3. Particle yields relative to protons (×100).

| Target and angle | 20-30 Mev |  | 30-40 Mev |  | 20-40 Mev |  |
|---|---|---|---|---|---|---|
|  | deuterons | tritons | deuterons | tritons | deuterons | tritons |
| Be $45^\circ$ | 9.0 ± 2.3 | 1.8 ± 1.1 | 14.3 ± 3.8 | 4.6 ± 1.8 | 10.7 ± 1.8 | 2.7 ± 0.9 |
| $90^\circ$ | 13.7 ± 2.8 | 5.8 ± 1.7 | 19.1 ± 4.0 | 3.3 ± 1.9 | 15.8 ± 2.2 | 4.8 ± 1.2 |
| $135^\circ$ | 20.6 ± 5.4 | 5.1 ± 3.0 | 12.2 ± 3.1 | 4.9 ± 1.8 | 16.2 ± 3.0 | 7.1 ± 1.8 |
| C $45^\circ$ | 8.1 ± 3.2 | 1.8 ± 1.6 | 10.0 ± 3.6 | 4.1 ± 1.3 | 8.9 ± 2.2 | 5.0 ± 1.5 |
| $90^\circ$ | 12.0 ± 2.8 | 3.3 ± 1.4 | 14.0 ± 4.0 | 2.3 ± 2.0 | 12.7 ± 2.2 | 3.0 ± 1.0 |
| $135^\circ$ | 10.8 ± 4.0 | 5.6 ± 2.3 | 13.8 ± 3.6 | 4.6 ± 1.9 | 11.1 ± 2.7 | 5.0 ± 1.5 |
| Pb $45^\circ$ | 28.8 ± 8.2 | 3.0 ± 3.0 | 17.4 ± 5.6 | 6.7 ± 3.2 | 22.8 ± 5.5 | 5.0 ± 2.3 |
| $90^\circ$ | 17.5 ± 4.1 | 7.2 ± 2.4 | 22.6 ± 5.1 | 2.5 ± 1.8 | 19.8 ± 3.1 | 5.1 ± 1.5 |
| $135^\circ$ | 21.9 ± 5.7 | 4.3 ± 2.3 | 14.5 ± 3.5 | 3.8 ± 1.6 | 18.0 ± 3.2 | 4.0 ± 1.4 |
| Pb $90^\circ$ 1/2 energy | 6.1 ± 3.6 | 0 ± 3.3 | 20.0 ± 9.0 | 3.3 ± 3.3 | 11.4 ± 4.0 | 1.3 ± 1.3 |

### E. Absolute value of differential cross sections

The following differential cross sections in μ barns/Q-Mev-steradian for 20-40 Mev particles at 90° to the 280 Mev beam have been computed:

| | Protons | Deuterons | Tritons | Total |
|---|---|---|---|---|
| Be | 1.21 ± 0.11 | 0.191 ± 0.027 | 0.058 ± 0.014 | 1.46 ± 0.11 |
| C | 2.47 ± 0.23 | 0.314 ± 0.055 | 0.074 ± 0.026 | 2.85 ± 0.24 |
| Pb | 17.2 ± 1.5 | 3.40 ± 0.99 | 0.89 ± 0.14 | 21.5 ± 1.8 |

(One Q, or equivalent quantum, corresponds to 280 Mev of photon energy; i.e., the number of Q is the energy in the beam divided by the maximum photon energy.) The beam monitor calibration for 320 Mev, $11.55 \times 10^7$ Q/mouse, has been used for the 280 Mev beam with the assumption that the error so introduced is not significant.

Corresponding weighted mean values for 20-40 Mev protons computed from the measurements of Levinthal and Silverman(24) are 7.89 μ barns/Mev-Q-steradian for Pb and 0.60 μ barns/Mev-Q-steradian for C. Comparison of the measurements at 70 Mev by these investigators with the measurements of Keck(25) indicate that their data may be low at least by a factor of four. This is in agreement within the uncertainty of the beam calibration (±30 percent) with the values calculated in this experiment for the sum of the cross sections for protons, deuterons, and tritons.

Variation of cross sections with atomic number is similar to that measured by Levinthal and Silverman.

## F. A/Z dependence

The d/p ratios measured at 90° for Be, C, and Pb, as well as the value published by De Wire for Cu are plotted in Fig. 11, against A/Z of the target nucleus. There appears to be a linear relationship, $d/p \propto A/Z$. As was indicated earlier, the d/p value reported by De Wire for Cu probably included some tritons.

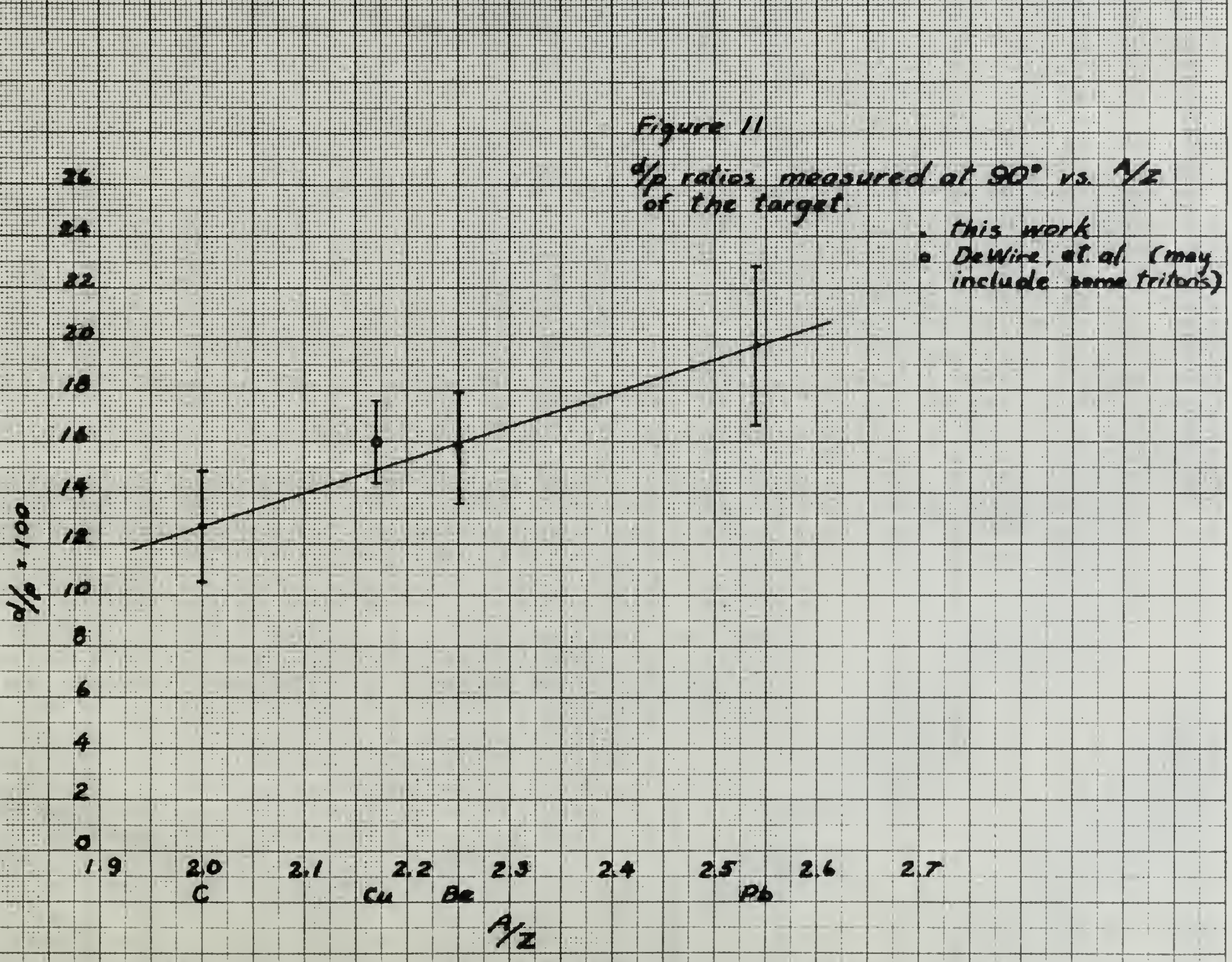

Figure 11

d/p ratios measured at 90° vs. A/Z of the target.

## V. CONCLUSIONS

To summarize the results of this experiment:

(1) Large deuteron and triton yields have been measured from widely dissimilar nuclides irradiated by 280 Mev bremsstrahlung.

(2) Both deuterons and tritons are found, though in smaller numbers relative to the protons, when the beam energy is reduced to 140 Mev.

(3) Angular distributions of protons, deuterons, and possibly tritons are roughly similar.

(4) There appears to be a linear relationship $d/p \propto A/Z$.

It will be shown that none of the above observations are inconsistent with a pick-up process for production of deuterons and tritons.

The deuteron and triton pick-up cross sections(9,10,11,13,14) measured by bombardment of nuclei with neutrons and protons indicate that the d/p and t/p ratios here reported are of the order of magnitude to be expected from this mechanism. A crude prediction of the d/p or t/p ratio to be expected from pick-up can be made by taking the ratio of the measured pick-up cross section to the total nuclear cross section. Such comparisons, of course, cannot be taken too seriously, since the two experiments are quite different. In one case a monoenergetic neutron

or proton beam is incident upon a nucleus in its ground state from which one particle is removed, while in the photonuclear reaction, the parent proton or neutron originates in the nucleus by some unspecified mechanism and possibly picks up a partner or partners from a highly excited assemblage of nucleons. Both the pick-up cross sections and the observed d/p ratios are energy dependent, and it is unfortunate that at this time there are no published experimental cross sections for deuteron and triton pick-up using bombarding particle energies in the range covered by this experiment.

Since both deuterons and tritons were observed using a maximum beam energy no greater than meson threshold, it is probable that mesonic effects do not play the dominant role in the photoproduction of these particles. A more convincing case could be made if more data had been obtained at reduced energy; however, the low intensity of the M.I.T. synchrotron beam at this energy made satisfactory exposures prohibitively long.

The similarities in the angular distributions of deuterons to those of protons of the same energy is consistent with a pick-up process, since in this process the deuterons are dragged along with the parent protons (and neutrons). A contribution from photomeson reabsorption, on the other hand, should be roughly isotropic.

The simple linear relationship of Fig. 10 between d/p ratios and A/Z tempts one to propose an equally simple explanation using the pick-up model.

It has been found experimentally$^{(24)}$ that photoproton yields are proportional to Z for particle energies considered here. Although less data are available on energetic photoneutrons, their yields seem to be similar to those of the protons. Therefore, assume

$$N_p = K_1 Z, \quad N_{pd} = (K_1 Z)P_{pd}$$

$$N_n = K_2 N, \quad N_{nd} = (K_2 N)P_{nd}$$

where $N_p$ and $N_n$ are the numbers of photoprotons and neutrons, respectively, $K_1$ and $K_2$ are proportionality constants, $P_{pd}$ and $P_{nd}$ are energy-dependent functions expressing the probabilities of proton-neutron and neutron-proton pick-up by an outgoing particle, and $N_{pd}$ and $N_{nd}$ are resulting numbers of deuterons formed. The deuteron-to-proton ratio then is

$$\frac{d}{p} = \frac{N_{pd} + N_{nd}}{N_p} = \frac{K_1 Z P_{pd} + K_2 N P_{nd}}{K_1 Z}$$

$$= P_{pd} + \frac{K_2}{K_1}\frac{N}{Z}P_{nd}$$

If, as is reasonable from the similarity in the measurements of York and Selove, we assume $P_{pd} \approx P_{nd}$, we get

$$\frac{d}{p} = Pd \left( \frac{Z + (K_2/K_1)N}{Z} \right)$$

If we further assume that $K_1 \approx K_2$, we get, finally

$$\frac{d}{p} \approx Pd\frac{A}{Z}$$

The nature of $P_{nd}$ and $P_{pd}$ should be considered further. It has been tacitly assumed in this development that the pick-up probabilities themselves do not vary with A. It might be reasonable to expect the Pd's to be proportional to the probability of a nuclear encounter which, for example, could be proportional to the nuclear radius, $R_o A^{1/3}$. This would predict that $\frac{d}{p} \propto \frac{A^{4/3}}{Z}$, in disagreement with the data. On the other hand, if the pick-up occurs only at the nuclear surface, as suggested by Chew and Goldberger,(12) $P_{nd}$ and $P_{pd}$ would depend on the nuclear surface densities of protons and neutrons respectively. Thus, more precise measurements of the d/p ratios over a wide range of nuclides might yield information both on the pick-up mechanism and on the nature of the nuclear surface.

## VI. EXTENSIONS OF PRESENT WORK

The results of this experiment suggest several further investigations:

(1) It would be desirable to extend the particle energy range investigated, using absorbers.

(2) The A/Z dependence indicated should be verified by irradiating additional target materials.

(3) More data should be obtained at low beam energies to reduce any mesonic contributions.

(4) Ranges of observation should be shifted to examine the doubly charged particles that are ejected and to determine the relative yields of $He^3$ and $He^4$.

This last point is particularly interesting because if tritons are formed by a pick-up process, some $He^3$ should be seen as well.

## VII. ACKNOWLEDGMENT

It is a pleasure to express my appreciation to Dr. J. W. Rosengren for the opportunity of performing my graduate research under his direction. His contributions included not only the equipment design but also a major share of the hard work in the conduct of the experiment.

# VIII. APPENDICES

## APPENDIX I

## DETECTION METHOD

For a heavy particle of charge Z, nonrelativistic energy E, and mass M, the rate of energy loss in a given material due to ionization(22) is

$$-\frac{dE}{dx} \sim \frac{Z^2}{v^2}\, g(v^2) \sim Z^2\left(\frac{M}{E}\right)h\left(\frac{E}{M}\right)$$

This may be written $dE/dx = aZ^2 f(M/E)$ where a is a constant. From the range-energy tables of Aron,(1) it may be seen that in Ag over a range of 10-150 Mev, $R \propto E^{1.73}$. (Ag is considered here since its stopping power most nearly approximates that of NaI.)

Differentiating, we get $dE/dx \sim 1/E^{0.73}$. Comparing this expression with the theoretical relation we obtain

$$\frac{dE}{dx} = aZ^2\left(\frac{M}{E}\right)^{0.73}$$

Thus, measurements of E and dE/dx suffice to identify the ionizing particle. For a given particle, the product $E \times (dE/dx) = aZ^2E^{0.17}M^{0.73}$, which is very nearly constant over a limited energy range; therefore a plot of dE/dx vs E should approximate a hyperbola.

For particles of the same energy,

$$\frac{(dE/dx)_{\text{deuteron}}}{(dE/dx)_{\text{proton}}} = 2^{0.73} = 1.66$$

and

$$\frac{(dE/dx)_{\text{triton}}}{(dE/dx)_{\text{proton}}} = 3^{0.73} = 2.23$$

# APPENDIX II.

## CHOICE OF NaI(Tl)

If the fluorescence efficiency, dL/dE, of a scintillation crystal is a function of the specific ionization, dE/dx, of the particle, we may write

$$\frac{dL}{dE} = g\left(\frac{dE}{dx}\right) \quad \text{or} \quad \frac{dL}{dx} = \frac{dE}{dx}g\left(\frac{dE}{dx}\right)$$

from Taylor et al,(23) for NaI(Tl) scintillators, $\frac{dL}{dx} \sim \frac{dE}{dx}$ for deuterons and protons with energies above 1 Kev. For anthracene, on the other hand, $\frac{dL}{dx}$ approaches $\left(\frac{dE}{dx}\right)^{0.62}$ in the limit at high energies. Therefore,

$$\frac{(dL/dx)_{\text{deuteron}}}{(dL/dx)_{\text{proton}}} = 2^{0.73} = 1.66 \quad \text{for a given energy (NaI)}$$

and $$\frac{(dL/dx)_{\text{deuteron}}}{(dL/dx)_{\text{proton}}} = \left(2^{0.73}\right)^{0.62} = 1.37 \text{ (anthracene).}$$

Thus NaI(Tl) is an inherently superior scintillator where particle identification is important.

# APPENDIX III

## RELATIVE MASS RESOLUTION

Considering statistical fluctuations alone, if the number of photoelectrons collected at the photocathode of counters No. 1 and No. 3 are $n_1 \Delta E$ and $n_3 E$, respectively, the relative pulse widths are $r_1 = \frac{1}{\sqrt{n_1 \Delta E}}$ and $r_3 = \frac{1}{\sqrt{n_3 E}}$, where n is the number of photoelectrons emitted per Mev lost in the crystal. From Appendix I, for particles of the same charge, $\frac{dE}{dx} \sim (\frac{m}{E})^{0.73}$, whence $m \sim E(\frac{dE}{dx})^{1.27}$.

Since $\Delta E \sim dE/dx$, we may write

$$m \sim E(\Delta E)^{1.27}$$

Thus the relative uncertainty in mass,

$$r_m = \sqrt{(r_{\Delta E^{1.27}})^2 + (r_E)^2}$$

$$= \sqrt{(1.27)^2 (r_{\Delta E})^2 + (r_E)^2}$$

Assuming statistical errors only, we substitute $r_1$ and $r_3$ for $r_{\Delta E}$ and $r_E$ to get

$$r_m = \sqrt{(1.27)^2 \frac{1}{n_1 \Delta E} + \frac{1}{n_3 E}} .$$

Since $E \geq 10\,\Delta E$, and $n_3 > n_1$, the second term under the radical can be neglected. When this is done, the variation in mass,

$$\Delta m = m r_m = \frac{1.27m}{\sqrt{n_1\,\Delta E}}$$

Substituting $\Delta E \simeq K(\frac{m}{E})^{0.73}$, we get

$$\Delta m = \frac{1.27m}{\left[n_1 K(m/E)^{0.73}\right]^{1/2}} = K'E^{0.36}m^{0.64}$$

where K and K' are constants. Therefore, the mass resolution of any particle relative to the mass resolution of a proton of the same energy is

$$\frac{\Delta m}{\Delta m_p} = (\frac{m}{m_p})^{0.64} \quad .$$

# IX. BIBLIOGRAPHY

(1) P. R. Byerly, Jr. and W. E. Stevens, Phys. Rev. 83, 54 (1951)

(2) W. H. Smith and L. J. Laslett, Phys. Rev. 86, 523 (1952).

(3) J. W. De Wire, H. Silverman, and B. Wolfe, Phys. Rev. 92, 519 (1953); Bull. Am. Phys. Soc. 29, 41 (1954)

(4) J. W. Blatt and V. F. Weisskopf, John Wiley and Sons, (1952)

(5) J. S. Levinger and H. A. Bethe, Phys. Rev. 85, 577 (1952)

(6) E. D. Courant, Phys. Rev. 82, 703 (1951)

(7) S. T. Butler, Proc. Roy. Soc. (London) A208, 559 (1951)

(8) S. T. Butler and E. E. Salpeter, Phys. Rev. 88, 133 (1952)

(9) H. F. York, Phys. Rev. 75, 1467 (1949)

(10) J. Hadley and H. F. York, Phys. Rev. 80, 345 (1950)

(11) W. Selove, Phys. Rev. 92, 1328 (1953)

(12) G. F. Chew and M. L. Goldberger, Phys. Rev. 77, 470 (1950)

(13) B. L. Cohen and T. H. Handley, Phys. Rev. 93, 514 (1954)

(14) G. L. Frye, Jr., Phys. Rev. 93, 1086 (1954)

(15) J. S. Levinger, Phys. Rev. 84, 43 (1951)

(16) A. G. W. Cameron, Phys. Rev. 86, 435 (1952)

(17) R. D. Miller, Phys. Rev. 82, 260 (1951)

(18) S. Kikuchi, Phys. Rev. 80, 492 (1950); ibid 83, 1255 (1951)

(19) J. G. Wilson, "Progress in Cosmic Ray Physics", Interscience Publishers, Inc., (1952)

(20) K. J. Le Couteur, Proc. Phys. Soc. (London) A63, 259 (1950)

(21) W. A. Aron, B. G. Hoffman, F. C. Williams, AECU-663 (revised 1949)

(22) B. Rossi, "High Energy Particles", Prentice-Hall, 1952.

(23) C. J. Taylor, W. K. Jentschke, M. E. Remley, F. S. Eby, and P. G. Kruger, Phys. Rev. 84, 1034 (1951)

(24) C. Levinthal and A. Silverman, Phys. Rev. 82, 822 (1951)

(25) J. C. Keck, Phys. Rev. 85, 410 (1952)

28841
Thesis
W47 Wertheim
Protons, deuterons, and tritons from photonuclear reactions.

Thesis
W47 Wertheim 28841
Protons, deuterons, and tritons from photonuclear reactions.

thesW47
Protons, deutrons, and tritos from photo
3 2768 001 95000 9
DUDLEY KNOX LIBRARY